Rapid Communications

Persistent correlation between superconductivity and antiferromagnetic fluctuations near a nematic quantum critical point in $FeSe_{1-x}S_x$

P. Wiecki,[1] K. Rana,[1] A. E. Böhmer,[1,2] Y. Lee,[1] S. L. Bud'ko,[1] P. C. Canfield,[1] and Y. Furukawa[1]

[1]*Ames Laboratory, U.S. DOE and Department of Physics and Astronomy, Iowa State University, Ames, Iowa 50011, USA*

[2]*Karlsruhe Institute of Technology, Institut für Festkörperphysik, 76021 Karlsruhe, Germany*

(Received 9 February 2018; revised manuscript received 12 July 2018; published 27 July 2018)

We present ^{77}Se-NMR measurements on $FeSe_{1-x}S_x$ samples with sulfur content $x = 0\%$, 9%, 15%, and 29%. Twinned nematic domains are observed in the NMR spectrum for all samples except $x = 29\%$. The NMR spin-lattice relaxation rate shows that antiferromagnetic (AFM) fluctuations are initially enhanced between $x = 0\%$ and $x = 9\%$, but are strongly suppressed for higher x values. The observed behavior of the AFM fluctuations parallels the superconducting transition temperature T_c in these materials, providing strong evidence for the primary importance of AFM fluctuations for superconductivity, despite the presence of nematic quantum criticality in the $FeSe_{1-x}S_x$ system.

DOI: 10.1103/PhysRevB.98.020507

Critical fluctuations of an ordered phase found in the proximity to unconventional superconductivity have frequently been discussed as a source of superconducting pairing [1–4]. In the iron-based superconductors [5,6], superconductivity (SC) is found in the vicinity of two types of long-range order: the stripe-type antiferromagnetic (AFM) order and the nematic order, which breaks the in-plane rotational symmetry while preserving time reversal symmetry. While dynamical AFM fluctuations are well known to support SC, experimental and theoretical studies have suggested that nematic fluctuations may also be important for high-T_c SC [7–9].

In this context, FeSe has emerged as a key material since it undergoes a nematic phase transition from a tetragonal to an orthorhombic structure at $T_s \approx 90$ K and develops superconductivity below $T_c \approx 8.5$ K, but does not display static magnetic ordering [10–12]. This suggests an opportunity to study the behavior of T_c near a nematic quantum critical point (QCP) isolated from a magnetic QCP. The nematic phase can be suppressed by pressure application, with T_s reaching 32 K at $p = 1.5$ GPa. However, an AFM ordered state emerges above $p = 0.8$ GPa [13,14] and merges with the nematic state above $p = 1.7$ GPa [15]. Nonmonotonic behavior of T_c is seen near the onset of the magnetic order [16], but overall T_c is strongly enhanced up to 37 K at $p = 6$ GPa [17–19]. While early nuclear magnetic resonance (NMR) measurements connected the enhancement of T_c to enhanced spin fluctuations under pressure [20], the recently revealed complexity of the phase diagram raises new questions. Notably, the role of nematic fluctuations in the superconductivity remains unclear.

The nematic phase can also be suppressed by S substitution in $FeSe_{1-x}S_x$ at ambient pressure, with the nematic phase disappearing around $x \approx 17\%$. Importantly, no long-range magnetic order can be observed at ambient pressure, which implies an isolated nematic QCP [21]. T_c initially increases slightly to $T_c \approx 10$ K at $x \approx 10\%$ [22] from $T_c \approx 8.5$ K at $x = 0\%$, but then decreases, reaching $T_c \approx 5$ K by $x = 29\%$. The application of pressure induces magnetic order in S-substituted samples [23,24].

Recent results have highlighted the rich interplay between magnetic, nematic, and superconducting orders in $FeSe_{1-x}S_x$. Elastoresistivity measurements found that nematic fluctuations diverge near the nematic QCP near $x \approx 17\%$ [21]. The full three-dimensional T-p-x dependent phase diagram revealed strongly enhanced T_c in regions lacking both nematic and AFM long-range orders [24]. Although several studies have suggested that T_c seems to not correlate with nematicity in $FeSe_{1-x}S_x$ [21,24–26], nematic fluctuations have been shown to strongly impact the SC pairing interactions [27]. Similarly, the SC gap structure is highly anisotropic in the ab plane [28], suggesting that nematicity is involved in the SC. However, no direct measurements of the concentration dependence of magnetic fluctuations have been reported yet.

Since magnetic fluctuations are considered to be one of the key ingredients for the appearance of SC in iron pnictides, it is crucial to reveal how magnetic fluctuations vary with S substitution in $FeSe_{1-x}S_x$. NMR is an ideal tool for the microscopic study of low-energy magnetic fluctuations in correlated electron systems. Here, we carried out ^{77}Se NMR measurements to investigate the static and dynamic magnetic properties of $FeSe_{1-x}S_x$. Our NMR data clearly show that stripe-type AFM fluctuations are initially slightly enhanced by S doping up to $x \approx 10\%$ from $x = 0\%$ but are strongly suppressed thereafter, particularly beyond the nematic dome above $x \approx 17\%$. This behavior shows a strong correlation with T_c, providing clear evidence for the primary importance of AFM fluctuations over critical nematic fluctuations for SC in $FeSe_{1-x}S_x$.

The crystals were grown using chemical vapor transport as outlined in Refs. [29,30]. The four different S-content crystals used are $x = 0$ ($T_s = 90$ K, $T_c = 8.5$ K), $x = 0.09$ ($T_s = 68$ K, $T_c = 10$ K), $x = 0.15$ ($T_s = 45$ K, $T_c = 8$ K), and $x = 0.29$ ($T_c = 5$ K). ^{77}Se NMR measurements have been carried out under a fixed magnetic external field of $H = 7.4089$ T applied either along the c axis or in the ab plane ([110] direction in the high-T tetragonal phase). The ab-plane orientation of the $x = 29\%$ crystals was not precisely controlled. At the NMR

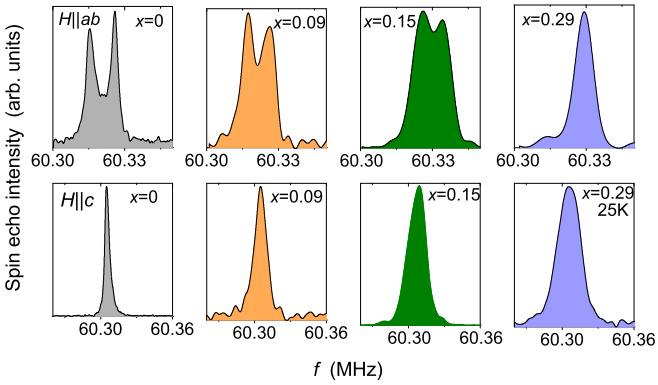

FIG. 1. Representative NMR spectra with $H \parallel ab$ (upper panels) and $H \parallel c$ (lower panels) at $T = 20$ K (unless otherwise specified) for indicated S concentrations x.

field with $H \parallel ab$, we observed $T_c(H) = 6.8$ K ($x = 0$), 7.8 K ($x = 0.09$), 7.25 K ($x = 0.15$), and $\leqslant$1.5 K ($x = 0.29$). Further experimental details are described in the Supplemental Material (SM) [30].

In FeSe, the single peak observed in the $H \parallel ab$ NMR spectrum at high T splits into two peaks below T_s due to nematic order, where the two peaks originate from twinned nematic domains [34–36]. Representative NMR spectra at 20 K for both field directions are shown in Fig. 1. Splittings of the $H \parallel ab$ spectra below T_s are also observed in $FeSe_{1-x}S_x$ for all samples in which a nematic transition was seen by resistivity [30].

The T dependence of the NMR shift K is shown in Fig. 2. As in FeSe, all K values increase monotonically with increasing T. K_{ab} is greater than K_c for all samples with almost no x dependence at low T. On the other hand, the high-T value of K shows a large concentration dependence, where K decreases with increasing x.

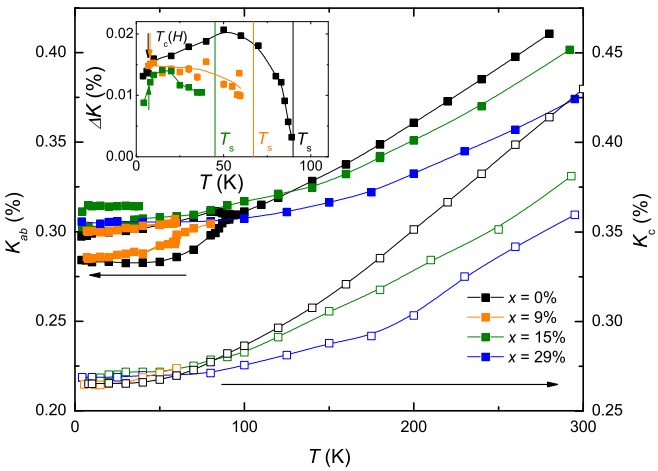

FIG. 2. T dependence of the NMR shift K for indicated x for $H \parallel ab$ (solid symbols) and $H \parallel c$ (open symbols). Inset: Splitting ΔK of the $H \parallel ab$ NMR spectrum. Vertical lines represent T_s from resistivity [30]. Arrows in the inset represent $T_c(H)$ from *in situ* ac susceptibility [30].

The inset of Fig. 2 shows the T and x dependence of the $H \parallel ab$ spectral splitting ΔK (the difference of the NMR shifts of the two peaks), which is a measure of the local nematic order parameter [34]. For FeSe, ΔK increases sharply below T_s and shows a broad maximum near ~50 K, as reported previously [34,36,37]. In contrast to FeSe, ΔK for $x = 9\%$ and $x = 15\%$ does not exhibit this maximum. While the ΔK of the $x = 0\%$ and $x = 9\%$ samples show no clear kinks at T_c, the $x = 15\%$ sample shows a noticeable drop in the SC state. In the S-doped samples, we could not resolve the splitting all the way up to the bulk T_s identified by resistivity measurements [30], likely due to the broadening of the two individual lines (see Fig. 1) by microscopic disorder from dopants and/or small variations in the local S composition. Due to the broad spectra relative to FeSe, no clear evidence for the local nematicity above T_s, observed in FeSe from FWHM measurements [36,38], could be found.

We now discuss the behavior of the low-energy magnetic fluctuations from NMR spin-lattice relaxation rate ($1/T_1$) data. $1/T_1T$ data are shown in Fig. 3 [39]. In general, $1/T_1T$ is related to the dynamical magnetic susceptibility as $1/T_1T \sim \gamma_N^2 k_B \sum_{\mathbf{q}} |A(\mathbf{q})|^2 \chi''(\mathbf{q}, \omega_N)/\omega_N$, where $A(\mathbf{q})$ is the wave-vector $\mathbf{q}$-dependent form factor and $\chi''(\mathbf{q}, \omega_N)$ is the imaginary part of $\chi(\mathbf{q}, \omega_N)$ at the Larmor frequency ω_N [40]. Above ~100 K, $1/T_1T$ shows a similar T dependence as $K(T)$ which measures the uniform susceptibility $\chi(\mathbf{q} = 0)$. In contrast, below ~100 K a strong upturn of $1/T_1T$ is observed

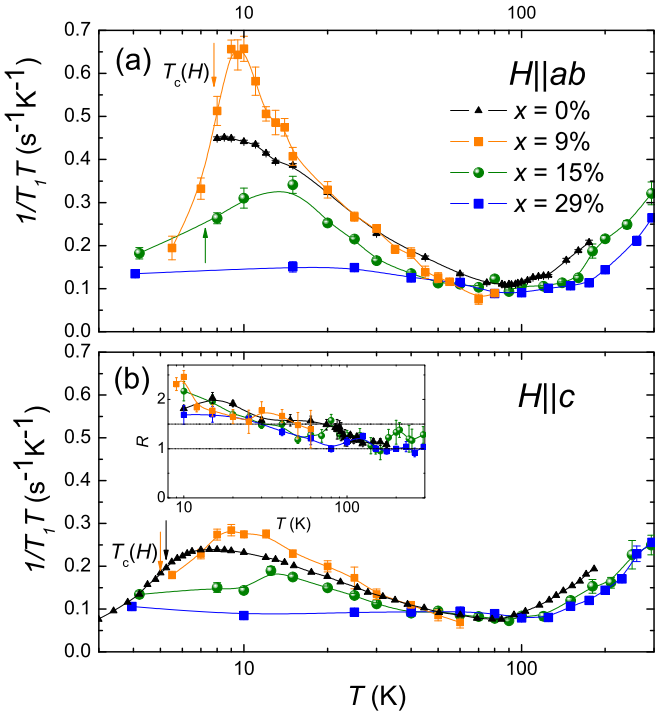

FIG. 3. T dependence of $1/T_1T$ for $H \parallel ab$ (upper panel) and $H \parallel c$ (lower panel) for indicated x. Arrows denote observed $T_c(H)$ from *in situ* ac susceptibility [30] (not shown for $x = 0\%$ $H \parallel ab$). For S-doped samples, missing arrows indicate $T_c(H) < 4.0$ K. Inset: The T dependence of $R = T_{1,c}/T_{1,ab}$ above T_c. Data for $x = 0\%$ (ab-plane average $1/T_1T$ and R at $H = 9$ T) from Ref. [35]. Data for $x = 0\%$ ($H \parallel c$ at $H = 7$ T) from Ref. [53].

which is not seen in $K(T)$. The enhancement of $1/T_1T$ at low T is therefore attributed to the growth of AFM spin fluctuations with $\mathbf{q} \neq 0$. The AFM fluctuations appear below ~100 K for all samples, but the enhancement of the AFM fluctuations shows a strong x dependence.

In order to characterize the AFM fluctuations, we plotted the ratio $R \equiv (1/T_1T)_{ab}/(1/T_1T)_c$ as shown in the inset of Fig. 3(b). According to previous NMR studies performed on Fe pnictides and related materials [41–46], R depends on the wave vector of the spin correlations. Assuming isotropic spin correlations, one expects $R = 1.5$ for stripe type, $R = 0.5$ for Néel type. $R \approx 1$ at high T and increases to $R > 1.5$ starting below ~100 K. The value of R observed here at low T is consistent with stripe-type spin correlations. The T dependence of R is independent of x within experimental error, indicating no change in the character of magnetic fluctuations with doping.

To discuss magnetic fluctuations in more detail, it is convenient to isolate the component-resolved hyperfine field (HF) fluctuations from the measured $1/T_1$ data. $1/T_1$ probes the $\mathbf{q}$ sum of fluctuations of HF at ω_N perpendicular to the applied field according to $(1/T_1)_{H\|i} = \gamma_N^2 \sum_{\mathbf{q}} [|H_j^{hf}(\mathbf{q}, \omega_N)|^2 + |H_k^{hf}(\mathbf{q}, \omega_N)|^2]$, where (i, j, k) are mutually orthogonal directions and $|H_j^{hf}(\mathbf{q}, \omega)|^2$ represents the $\mathbf{q}$-dependent power spectral density of the jth component of HF at the nuclear site. Therefore, we define the quantities $1/T_{1,\perp} \equiv (1/T_1)_{H\|c} = 2\gamma_N^2 \sum_{\mathbf{q}} |H_{ab}^{hf}(\mathbf{q}, \omega_N)|^2$ and $1/T_{1,\|} \equiv 2(1/T_1)_{H\|ab} - (1/T_1)_{H\|c} = 2\gamma_N^2 \sum_{\mathbf{q}} |H_c^{hf}(\mathbf{q}, \omega_N)|^2$ [33]. Note that, for simplicity, we have neglected any ab-plane anisotropy due to nematicity ($H_a^{hf} = H_b^{hf} \equiv H_{ab}^{hf}$). Thus defined, $1/T_{1,\perp}$ ($1/T_{1,\|}$) directly measures the ab (c) component of HF fluctuations $\sum_{\mathbf{q}} |H_{ab}^{hf}(\mathbf{q}, \omega_N)|^2$ ($\sum_{\mathbf{q}} |H_c^{hf}(\mathbf{q}, \omega_N)|^2$).

In Fermi-liquid systems, one expects that $1/T_1T \propto K_{spin}^2$. Here, $K_{spin} = K - K_0$, where K_0 is the T-independent chemical shift (see [30]). K_{spin} probes the uniform $\mathbf{q} = 0$ susceptibility according to $K_{spin,i} = A_{ii}\chi_{ii}(0)$, where A_{ii} is the hyperfine coupling constant. Therefore, to examine the contribution of $\mathbf{q} \neq 0$ correlations one can compare $1/T_1T$ to K_{spin}^2. The quantities $1/T_{1,\|}T$ and $1/T_{1,\perp}T$ should be compared to $K_{spin,c}^2$ and $K_{spin,ab}^2$, respectively [33]. The experimentally observed $1/T_1T$ can then be decomposed into $\mathbf{q} = 0$ and AFM ($\mathbf{q} \neq 0$) components as $1/T_1T = (1/T_1T)_{AFM} + (1/T_1T)_{\mathbf{q}=0}$. We have $(1/T_1T)_{\mathbf{q}=0} = CK_{spin}^2$, where C is a proportionality constant determined empirically from the high-T data [30].

In Fig. 4, we compare the angle-resolved pairs of $1/T_1T$ and CK_{spin}^2. Above ~100 K, it is clear that $1/T_1T \approx CK_{spin}^2$, indicating that the T_1 relaxation is driven by the $\mathbf{q} = 0$ component. In contrast, the difference between $1/T_1T$ and CK_{spin}^2 can be clearly seen below ~100 K and is attributed to the contribution of AFM fluctuations $(1/T_1T)_{AFM}$.

Relative to FeSe, spin fluctuations are enhanced at $x = 9\%$, slightly suppressed at $x = 15\%$, and strongly suppressed for $x = 29\%$. The x dependence of the AFM fluctuation enhancement closely parallels the x dependence of T_c, which shows a slight enhancement between $x = 0\%$ and $x = 9\%$ and is suppressed at higher doping levels. The suppression of magnetic fluctuations for $x \geqslant 15\%$ is consistent

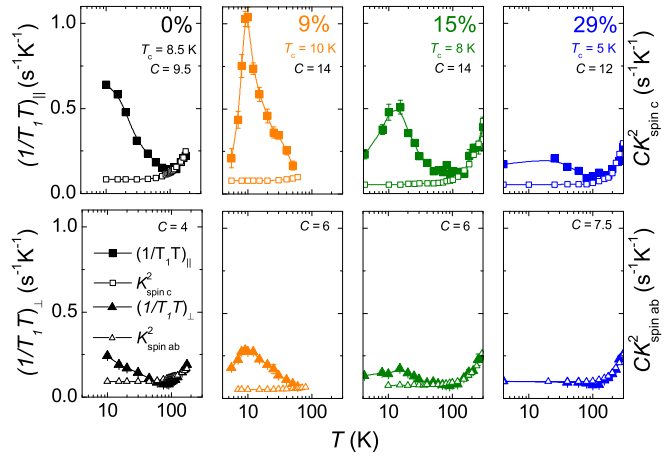

FIG. 4. Comparison of $1/T_1T$ (left axes, solid symbols) with CK_{spin}^2 (right axes, open symbols) for indicated x. The upper panels compare $1/T_{1,\|}T$ to $CK_{spin,c}^2$, while the lower panels compare $1/T_{1,\perp}T$ to $CK_{spin,ab}^2$. The empirical value of C (in units of 10^4 s^{-1} K^{-1}) for each panel is indicated.

with angle-resolved photoemission spectroscopy (ARPES) data [47].

In all cases, we find that $1/T_{1,\|}T > 1/T_{1,\perp}T$ at low T, indicating that $\sum_{\mathbf{q}} |H_c^{hf}(\mathbf{q}, \omega_N)|^2$ is greater than $\sum_{\mathbf{q}} |H_{ab}^{hf}(\mathbf{q}, \omega_N)|^2$. The HF at the Se nuclear site is determined from the magnetic moments on the Fe sites by the hyperfine coupling tensor. Since the stripe-type AFM fluctuations produce the HF fluctuations at the Se site through off-diagonal components of the hyperfine coupling tensor [6,48], the fact that $|H_c^{hf}|^2$ is greater than $|H_{ab}^{hf}|^2$ shows that the ab-plane polarized stripe-type AFM fluctuations are more developed than the corresponding c-axis polarized fluctuations, similar to the $BaFe_2As_2$ system [33].

Within an itinerant picture, the change in the AFM correlations with doping would be associated with a change in the nesting condition due to modification of the Fermi surface with S substitution. To understand the band structure of $FeSe_{1-x}S_x$, we performed electronic structure calculations [49] using the full-potential linearized augmented plane-wave method [50] with a generalized gradient approximation [51]. Here, we calculate the band structure for the tetragonal phases in $FeSe_{1-x}S_x$ using an FeSe unit cell, adopting chemical pressure effects on the a and c lattice parameters. The calculated band dispersion is shown in Fig. 5(a), which is in good agreement with the previous report [25]. The calculated Fermi surface has three hole pockets around the Γ point and two electron pockets at the M point along the [110] direction [Fig. 5(b)]. We find that the size of the smallest of the three hole pockets, originating from the d_{xy} orbital, is increased by S doping. In contrast, the other pockets, originating from d_{yz} and d_{zx} orbitals, do not change. These results continue to hold for a 1% reduction of the chalcogen height, which also occurs by S doping [24]. Thus the d_{xy} orbital can be considered to play an important role in AFM spin correlations and also in the appearance of SC in $FeSe_{1-x}S_x$.

Finally, let us comment on the temperature dependence of $1/T_1T$ observed in $x = 9\%$ and $x = 15\%$ (see Fig. 3). For

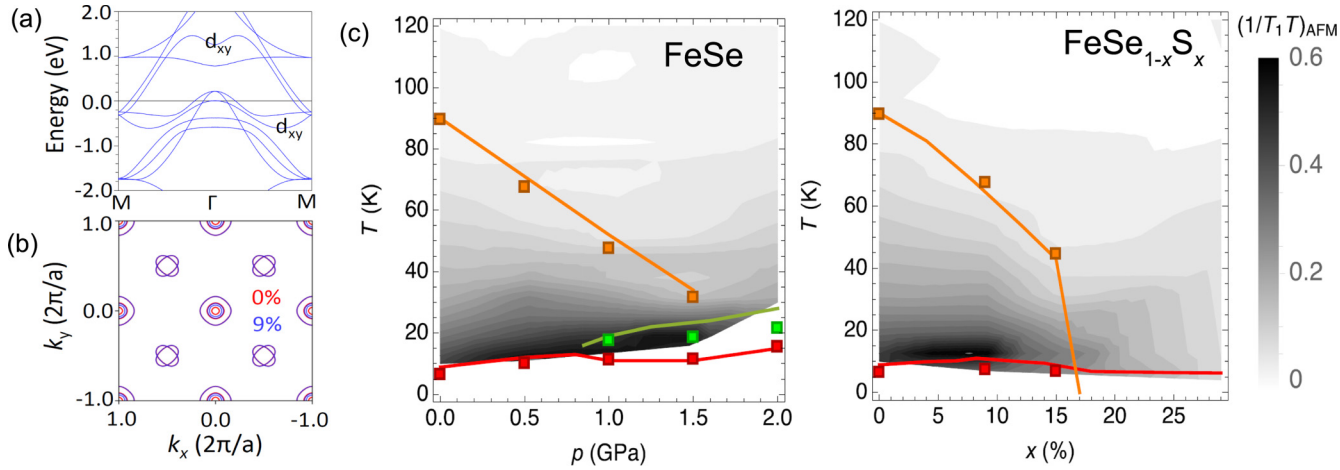

FIG. 5. (a) Band dispersion of FeSe in the tetragonal phase, with bands of d_{xy} orbital character indicated. (b) Cross sections of the Fermi surface in the tetragonal phase at $k_z = 0$ for $x = 0\%$ (red) and $x = 9\%$ (blue). (c) Comparison of AFM fluctuations in FeSe under pressure [36] (left panel) and $FeSe_{1-x}S_x$ (right panel). Here, the AFM contribution to $1/T_1T$ is defined by $(1/T_1T)_{\rm AFM} \equiv (1/T_1T) - (1/T_1T)_{\mathbf{q}=0}$ using $H \parallel ab$ data [30]. Solid lines show T_s (orange), T_N (green), and T_c (red) from resistivity at $H = 0$ [13,16,23,47]. Data points show T_s, T_N, and $T_c(H)$ from NMR under $H \sim 7.4$ T (this work and Ref. [36]). Note $T_c(H)$ for $x = 29\%$ is less than 1.5 K.

$x = 0\%$, the maximum of $1/T_1T$ has been reported to occur close to T_c [34,37]. However, for $x = 9\%$ and $x = 15\%$, we find that the maximum of $1/T_1T$ instead occurs well above $T_c(H)$, as determined by our *in situ* ac-susceptibility measurements [30]. At $x = 9\%$, we find $T_c(H \parallel ab) = 7.8$ K and $T_c(H \parallel c) = 5.0$ K, while $1/T_1T$ peaks at ~9 K for both H directions. At $x = 15\%$, we find $T_c(H \parallel ab) = 7.25$ K and $T_c(H \parallel c) \leqslant 4.0$ K. However, for both H directions, $1/T_1T$ peaks at ~12–15 K. These results imply a suppression of magnetic fluctuations just above T_c in the S-doped samples. The effect is more apparent for $H \parallel c$ data. Furthermore, the T difference between T_c and the peak of $1/T_1T$ appears to increase with doping. Similar behavior has been observed in FeSe and discussed in terms of a possible SC fluctuation effect [52,53]. Reductions of $1/T_1T$ above T_c have been observed in $LaFeAsO_{1-x}F_x$ [42,54] and $Ca(Fe_{1-x}Co_x)_2As_2$ [55] where pseudogap behavior has been discussed. Detailed H-dependent measurements on the S-doped samples will be needed to confirm the origin of the suppression of $1/T_1T$.

Our main results are summarized in the phase diagram of Fig. 5(c), which shows a contour plot of the AFM contribution to $1/T_1T$ as a function of x and T. For comparison, a similar plot for FeSe under pressure is also shown. In both cases, the bulk nematic order is suppressed. In FeSe, AFM fluctuations are roughly independent of pressure or slightly enhanced [36]. In $FeSe_{1-x}S_x$, the AFM fluctuations are strongly suppressed by S doping after an initial slight enhancement for $x \approx 9\%$, where the AFM fluctuations are strongly correlated with T_c. In contrast, nematic fluctuations are most strongly enhanced near the nematic QCP at $x \approx 17\%$ [21] and show no correlation with T_c. These NMR results clearly demonstrate the primary importance of AFM fluctuations to SC in $FeSe_{1-x}S_x$, and help to disentangle the roles of magnetic and nematic fluctuations in iron-based superconductors in general.

Note added. Quite recently, a different x dependence of T_c has been reported in $FeSe_{1-x}S_x$ crystals where T_c keeps increasing up to $x \sim 0.15$ [56]. It is interesting to perform NMR measurements to investigate how the magnetic fluctuations change in the crystals. This would be a future project.

The research was supported by the US Department of Energy, Office of Basic Energy Sciences, Division of Materials Sciences and Engineering. Ames Laboratory is operated for the US Department of Energy by Iowa State University under Contract No. DE-AC02-07CH11358.

[1] D. J. Scalapino, Rev. Mod. Phys. **84**, 1383 (2012).
[2] N. J. Curro, T. Caldwell, E. D. Bauer, L. A. Morales, M. J. Graf, Y. Bang, A. V. Balatsky, J. D. Thompson, and J. L. Sarrao, Nature (London) **434**, 622 (2005).
[3] T. Hattori, Y. Ihara, Y. Nakai, K. Ishida, Y. Tada, S. Fujimoto, N. Kawakami, E. Osaki, K. Deguchi, N. K. Sato, and I. Satoh, Phys. Rev. Lett. **108**, 066403 (2012).
[4] E. Bertel and A. Menzel, Symmetry **8**, 45 (2016).
[5] P. C. Canfield and S. L. Bud'ko, Annu. Rev. Condens. Matter Phys. **1**, 27 (2010).
[6] D. C. Johnston, Adv. Phys. **59**, 803 (2010).
[7] H.-H. Kuo, J.-H. Chu, J. C. Palmstrom, S. A. Kivelson, and I. R. Fisher, Science **352**, 958 (2016).
[8] S. Lederer, Y. Schattner, E. Berg, and S. A. Kivelson, Phys. Rev. Lett. **114**, 097001 (2015).
[9] S. Lederer, Y. Schattner, E. Berg, and S. A. Kivelson, Proc. Natl. Acad. Sci. USA **114**, 4905 (2017).
[10] F.-C. Hsu, J.-Y. Luo, K.-W. Yeh, T.-K. Chen, T.-W. Huang, P. M. Wu, Y.-C. Lee, Y.-L. Huang, Y.-Y. Chu, D.-C. Yan, and M.-K. Wu, Proc. Natl. Acad. Sci. USA **105**, 14262 (2008).
[11] T. M. McQueen, A. J. Williams, P. W. Stephens, J. Tao, Y. Zhu, V. Ksenofontov, F. Casper, C. Felser, and R. J. Cava, Phys. Rev. Lett. **103**, 057002 (2009).
[12] A. E. Böhmer and A. Kreisel, J. Phys.: Condens. Matter **30**, 023001 (2018).

[13] T. Terashima, N. Kikugawa, S. Kasahara, T. Watashige, T. Shibauchi, Y. Matsuda, T. Wolf, A. E. Böhmer, F. Hardy, C. Meingast, H. v. Löhneysen, and S. Uji, J. Phys. Soc. Jpn. **84**, 063701 (2015).

[14] M. Bendele, A. Amato, K. Conder, M. Elender, H. Keller, H.-H. Klauss, H. Luetkens, E. Pomjakushina, A. Raselli, and R. Khasanov, Phys. Rev. Lett. **104**, 087003 (2010).

[15] K. Kothapalli, A. E. Böhmer, W. T. Jayasekara, B. G. Ueland, P. Das, A. Sapkota, V. Taufour, Y. Xiao, E. Alp, S. L. Bud'ko, P. C. Canfield, A. Kreyssig, and A. I. Goldman, Nat. Commun. **7**, 12728 (2016).

[16] U. S. Kaluarachchi, V. Taufour, A. E. Böhmer, M. A. Tanatar, S. L. Bud'ko, V. G. Kogan, R. Prozorov, and P. C. Canfield, Phys. Rev. B **93**, 064503 (2016).

[17] Y. Mizuguchi, F. Tomioka, S. Tsuda, T. Yamaguchi, and Y. Takano, Appl. Phys. Lett. **93**, 152505 (2008).

[18] S. Margadonna, Y. Takabayashi, Y. Ohishi, Y. Mizuguchi, Y. Takano, T. Kagayama, T. Nakagawa, M. Takata, and K. Prassides, Phys. Rev. B **80**, 064506 (2009).

[19] S. Medvedev, T. M. McQueen, I. A. Troyan, T. Palasyuk, M. I. Eremets, R. J. Cava, S. Naghavi, F. Casper, V. Ksenofontov, G. Wortmann, and C. Felser, Nat. Mater. **8**, 630 (2009)

[20] T. Imai, K. Ahilan, F. L. Ning, T. M. McQueen, and R. J. Cava, Phys. Rev. Lett. **102**, 177005 (2009).

[21] S. Hosoi, K. Matsuura, K. Ishida, H. Wang, Y. Mizukami, T. Watashige, S. Kasahara, Y. Matsuda, and T. Shibauchi, Proc. Natl. Acad. Sci. USA **113**, 8139 (2016).

[22] M. Abdel-Hafiez, Y.-Y. Zhang, Z.-Y. Cao, C.-G. Duan, G. Karapetrov, V. M. Pudalov, V. A. Vlasenko, A. V. Sadakov, D. A. Knyazev, T. A. Romanova, D. A. Chareev, O. S. Volkova, A. N. Vasiliev, and X.-J. Chen, Phys. Rev. B **91**, 165109 (2015).

[23] L. Xiang, U. S. Kaluarachchi, A. E. Böhmer, V. Taufour, M. A. Tanatar, R. Prozorov, S. L. Bud'ko, and P. C. Canfield, Phys. Rev. B **96**, 024511 (2017).

[24] K. Matsuura, Y. Mizukami, Y. Arai, Y. Sugimura, N. Maejima, A. Machida, T. Watanuki, T. Fukuda, T. Yajima, Z. Hiroi, K. Y. Yip, Y. C. Chan, Q. Niu, S. Hosoi, K. Ishida, K. Mukasa, T. Watashige, S. Kasahara, J.-G. Cheng, S. K. Goh *et al.*, Nat. Commun. **8**, 1143 (2017).

[25] M. D. Watson, T. K. Kim, A. A. Haghighirad, S. F. Blake, N. R. Davies, M. Hoesch, T. Wolf, and A. I. Coldea, Phys. Rev. B **92**, 121108(R) (2015).

[26] A. I. Coldea, S. F. Blake, S. Kasahara, A. A. Haghighirad, M. D. Watson, W. Knafo, E. S. Choi, A. McCollam, P. Reiss, T. Yamashita, M. Bruma, S. Speller, Y. Matsuda, T. Wolf, T. Shibauchi, and A. J. Schofield, arXiv:1611.07424.

[27] Y. Sato, S. Kasahara, T. Taniguchi, X. Xing, Y. Kasahara, Y. Tokiwa, Y. Yamakawa, H. Kontani, T. Shibauchi, and Y. Matsuda, Proc. Natl. Acad. Sci. USA **115**, 1227 (2018).

[28] P. Sprau, A. Kostin, A. Kreisel, A. E. Böhmer, V. Taufour, P. C. Canfield, S. Mukherjee, P. J. Hirschfeld, B. M. Andersen, and J. C. Davis, Science **357**, 75 (2017).

[29] A. E. Böhmer, V. Taufour, W. E. Straszheim, T. Wolf, and P. C. Canfield, Phys. Rev. B **94**, 024526 (2016).

[30] See Supplemental Material at http://link.aps.org/supplemental/10.1103/PhysRevB.98.020507 for the sample growth and characterization, the experimental details, the scaling analysis of $1/T_1T$ and $K^2_{\rm spin}$, and the contour plot of $(1/T_1T)_{\rm AFM}$ and K-χ plot analysis, which includes Refs. [31,32,33].

[31] X. Lai, H. Zhang, Y. Wang, X. Wang, X. Zhang, J. Lin, and F. Huang, J. Am. Chem. Soc. **137**, 10148 (2015).

[32] M. A. Tanatar, A. E. Böhmer, E. I. Timmons, M. Schütt, G. Drachuck, V. Taufour, K. Kothapalli, A. Kreyssig, S. L. Bud'ko, P. C. Canfield, R. M. Fernandes, and R. Prozorov, Phys. Rev. Lett. **117**, 127001 (2016).

[33] P. Wiecki, B. Roy, D. C. Johnston, S. L. Bud'ko, P. C. Canfield, and Y. Furukawa, Phys. Rev. Lett. **115**, 137001 (2015).

[34] S.-H. Baek, D. V. Efremov, J. M. Ok, J. S. Kim, J. van den Brink, and B. Büchner, Nat. Mater. **14**, 210 (2015).

[35] A. E. Böhmer, T. Arai, F. Hardy, T. Hattori, T. Iye, T. Wolf, H. V. Löhneysen, K. Ishida, and C. Meingast, Phys. Rev. Lett. **114**, 027001 (2015).

[36] P. Wiecki, M. Nandi, A. E. Böhmer, S. L. Bud'ko, P. C. Canfield, and Y. Furukawa, Phys. Rev. B **96**, 180502(R) (2017).

[37] P. S. Wang, S. S. Sun, Y. Cui, W. H. Song, T. R. Li, R. Yu, H. Lei, and W. Yu, Phys. Rev. Lett. **117**, 237001 (2016).

[38] P. S. Wang, P. Zhou, S. S. Sun, Y. Cui, T. R. Li, H. Lei, Z. Wang, and W. Yu, Phys. Rev. B **96**, 094528 (2017).

[39] Here, $(1/T_1T)_{H\|ab}$ is averaged over any ab-plane anisotropy due to nematicity [30].

[40] A. Smerald and N. Shannon, Phys. Rev. B **84**, 184437 (2011).

[41] K. Kitagawa, N. Katayama, K. Ohgushi, and M. Takigawa, J. Phys. Soc. Jpn. **78**, 063706 (2009).

[42] S. Kitagawa, Y. Nakai, T. Iye, K. Ishida, Y. Kamihara, M. Hirano, and H. Hosono, Phys. Rev. B **81**, 212502 (2010).

[43] M. Hirano, Y. Yamada, T. Saito, R. Nagashima, T. Konishi, T. Toriyama, Y. Ohta, H. Fukazawa, Y. Kohori, Y. Furukawa, K. Kihou, C.-H. Lee, A. Iyo, and H. Eisaki, J. Phys. Soc. Jpn. **81**, 054704 (2012).

[44] Y. Furukawa, B. Roy, S. Ran, S. L. Bud'ko, and P. C. Canfield, Phys. Rev. B **89**, 121109(R) (2014).

[45] A. Pandey, D. G. Quirinale, W. Jayasekara, A. Sapkota, M. G. Kim, R. S. Dhaka, Y. Lee, T. W. Heitmann, P. W. Stephens, V. Ogloblichev, A. Kreyssig, R. J. McQueeney, A. I. Goldman, A. Kaminski, B. N. Harmon, Y. Furukawa, and D. C. Johnston, Phys. Rev. B **88**, 014526 (2013).

[46] Q.-P. Ding, P. Wiecki, V. K. Anand, N. S. Sangeetha, Y. Lee, D. C. Johnston, and Y. Furukawa, Phys. Rev. B **93**, 140502 (2016).

[47] P. Reiss, M. D. Watson, T. K. Kim, A. A. Haghighirad, D. N. Woodruff, M. Bruma, S. J. Clarke, and A. I. Coldea, Phys. Rev. B **96**, 121103(R) (2017).

[48] K. Kitagawa, N. Katayama, K. Ohgushi, M. Yoshida, and M. Takigawa, J. Phys. Soc. Jpn. **77**, 114709 (2008).

[49] To obtain the self-consistent charge density, we employed muffin-tin radii $R_{\rm MT} = 2.0$ a.u. for Fe and Se, respectively, and $R_{\rm MT}k_{\rm max} = 8.0$ and which set the maximum k value in the expansion of plane waves. The Se atom position was relaxed until the force on the Se atom was less than 0.1 mRy/a.u. Calculations were iterated, with 4800 k points for whole Brillouin zone, to reach the total energy convergence criterion that was 0.01 mRy/cell. For the Fermi-surface calculations, we chose the $k_z = 0.0(2\pi/c)$ plane and divided the $-2\pi/a \leqslant k_x, k_x \leqslant 2\pi/a$ region by a 200×220 mesh that resulted in 40 401 k points.

[50] P. Blaha, K. Schwarz, G. K. H. Madsen, D. Kvasnick, and J. Luitz, *WIEN2K, An Augmented Plane Wave+Local Orbitals Program for Calculation Crystal Properties* (Karlheinz Schwarz, Technical Universität Wien, Austria, 2001).

[51] J. P. Perdew, K. Burke, and M. Ernzerhof, Phys. Rev. Lett. **77**, 3865 (1996).

[52] S. Kasahara, T. Yamashita, A. Shi, R. Kobayashi, Y. Shimoyama, T. Watashige, K. Ishida, T. Terashima, T Wolf, F. Hardy, C. Meingast, H. V. Löhneysen, A. Levchenko, T. Shibauchi, and Y. Matsuda, Nat. Commun. **7**, 12843 (2016).

[53] A. Shi, T. Arai, S. Kitagawa, T. Yamanaka, K. Ishida, A. E. Böhmer, C. Meingast, T. Wolf, M. Hirata, and T. Sasaki, J. Phys. Soc. Jpn. **87**, 013704 (2018).

[54] T. Oka, Z. Li, S. Kawasaki, G. F. Chen, N. L. Wang, and G.-Q. Zheng, Phys. Rev. Lett. **108**, 047001 (2012).

[55] J. Cui, B. Roy, M. A. Tanatar, S. Ran, S. L. Bud'ko, R. Prozorov, P. C. Canfield, and Y. Furukawa, Phys. Rev. B **92**, 184504 (2015).

[56] D. Chareev, Y. Ovchenkov, L. Shvanskaya, A. Kovalskii, M. Abdel-Hafiez, D. J. Trainer, E. M. Lechner, M. Iavarone, O. Volkova, and A. Vasiliev, CrystEngComm **20**, 2449 (2018).